STRUCTURAL AND MAGNETIC ORDERING IN BULK Sr_2FeMoO_6 SYNTHESIZED BY PLANETARY BALL MILL: THE EFFECTS OF GRINDING

A Thesis

Presented in Partial Fulfillment of the Requirement for the

Degree Bachelor of Science With Distinction in the

Graduate School of The Ohio State University

By

Jeremy Matthew Lucy

******

The Ohio State University

2011

Thesis Examination Committee:

Approved by

Professor Fengyuan Yang, Adviser

Professor Patricia Morris

Michael Mason

Adviser

Department of Engineering

ABSTRACT

The standard solid-state synthesis procedure has been widely used to make bulk complex oxides, including the half-metallic double perovskite Sr_2FeMoO_6. However, although it is generally recognized that multi-step grinding and heating are crucial for synthesis of high quality materials, little has been done to quantitatively characterize the effects of grinding on the qualities of the final products. We systematically varied the level of grinding, ranging from poor grinding by hand for a short period of time to very fine grinding and mixing by a planetary ball mill for many hours which produces uniform sub-micron particles. X-Ray Diffraction, Scanning Electron Microscopy, and Superconducting Quantum Interference Device magnetometry were used to characterize the structural and magnetic properties. The Sr_2FeMoO_6 samples made by different grinding methods exhibit drastically different structural and magnetic ordering. The highest quality Sr_2FeMoO_6 is from the most thorough grinding and gives a close to ideal Fe/Mo ordering and magnetic moment close to 4 Bohr magnetron per formula unit.

Dedicated to my family and to those mentors who
have inspired me to pursue a career in the natural sciences

ACKNOWLEDGMENTS

I wish to thank my adviser, Professor Fengyuan Yang, for his support over the past four years. He has provided me the resources necessary to conduct inspiring research and to lead me toward a path of success.

I am grateful for the help I have received along the way from a good friend and co-worker, Dr. Adam Hauser. His advice continues to guide and challenge me in my growth as a scholar.

I thank all those who have provided me experimental support in my research including Graduate Associate Brian Peters and students of those laboratories used for materials analyses.

I also wish to thank my father, Ronnie Towe, and teacher, Steve Brickner, who both inspired me in my early drive toward the fields of Engineering and Physics.

This work has been supported by the Center for Emergent Materials, a National Science Foundation Materials Research Science and Engineering Center at The Ohio State University (DMR-0820414).

VITA

October 12, 1988….……..Born – Cincinnati, Ohio, United States

Summer 2010……Undergraduate Researcher, Cornell University

2007-present...……..Undergraduate Researcher, The Ohio State University

PUBLICATIONS

Research Publication Contributions

1. Hauser A.J., Williams R.E.A., Ricciardo R.A., Genc A., Dixit M., Lucy J.M., Woodward P.M., Fraser H.L., Yang F.Y., "Unlocking the potential of half-metallic Sr_2FeMoO_6 films through controlled stoichiometry and double-perovskite ordering." Phys. Rev. B, **83**, 014407, (2011).

2. Pak J., Lin W., Wang K., Chinchore A., Shi M., Ingram D.C., Smith A.R., Sun K., Lucy J.M., Hauser A.J., Yang F.Y., "Growth of epitaxial iron nitride ultrathin film on zinc-blende gallium nitride." J. Vac. Sci. & Tech., **28**, 536-540, (2010).

FIELD OF STUDY

Major Field: Engineering Physics
Specialization: Materials Science and Engineering

TABLE OF CONTENTS

LIST OF TABLES

LIST OF FIGURES

CHAPTER 1

INTRODUCTION

The Center for Emergent Materials (CEM) is a National Science Foundation (NSF) Materials Research Science and Engineering Center (MRSEC) at The Ohio State University. Two Interdisciplinary Research Groups (IRGs) serve significant roles in the MRSEC. IRG-1 specializes in research on spin-preserving networks for next-generation information processing, specifically studying spin injection and extraction. IRG-2, the group my research project is a part of, focuses on the synthesis and analysis (both experimental and theoretical) of double perovskite materials, their interfaces, and heterostructures of such materials.

As a part of IRG-2, the research conducted in Professor Yang's laboratory is focused on the experimental synthesis and analysis of complex double perovskites. Our group uses refined solid-state synthesis techniques to chemically synthesize bulk double perovskite materials and uses such bulk materials in pressed bulk targets used in ultra-high vacuum magnetron sputtering. Ultra-high vacuum magnetron sputtering is an epitaxial film growth technique which uses transfer of kinetic energy from gas atoms to a target material in order to energetically expel the material in the form of plasma. The plasma material can then be deposited on substrate materials. Ultra-high vacuum

magnetron sputtering is demonstrated in Figure 1 below. The magnetic field above the target material serves to keep electrons close to the surface of the material where energy transfer takes place. A negative potential bias is applied to the target so that positively charged Ar ions are attracted toward the target.

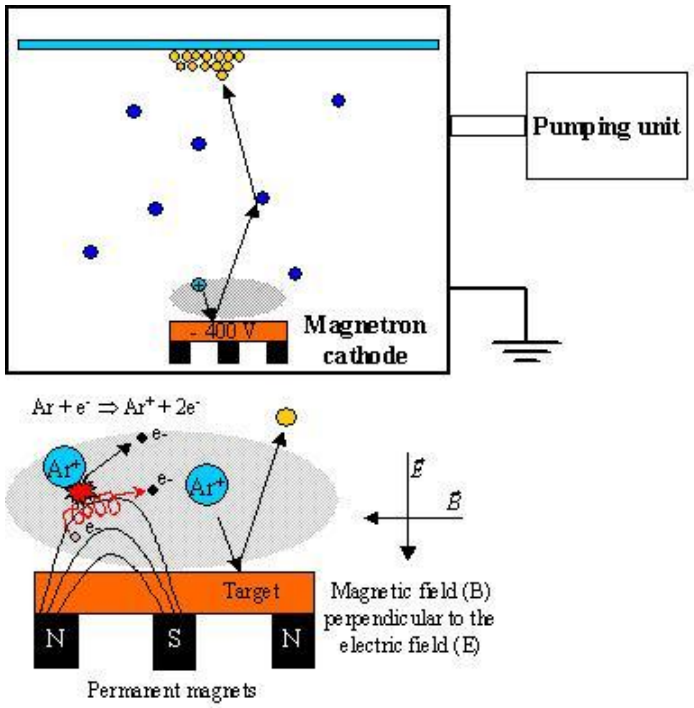

Figure 1.1: Schematic of the ultra-high vacuum magnetron sputtering process. http://lermps.utbm.fr/upload/gestionFichiers/pvdfig5_328.jpg

After epitaxial films are grown in the laboratory, those films are analyzed structurally, thermally, electronically, and magnetically through the use of techniques such as X-Ray Diffraction (XRD), thermogravimetric analysis (TGA), point contact Andreev reflection (PCAR), and magnetometry, respectively.

The project discussed in this document focuses on the effects of grinding variations during bulk synthesis on the properties of a double perovskite, Sr_2FeMoO_6, in its bulk form.

CHAPTER 2

INTEREST IN DOUBLE PEROVSKITES AND Sr_2FeMoO_6

The general structure for double perovskite, $A_2BB'O_6$, materials is shown in Figure 2.1 (left), where A is typically a group II metal and B/B' are transition metals. Also in Figure 2.1 (right), it is demonstrated how the B and B' site elements can be chosen from a variety of choices. Depending on the identities of the A (typically Sr^{2+}, Ca^{2+}, or Ba^{2+}), B, and B' site elements, double perovskite materials can exhibit an extraordinary range of properties. These tailored materials can be ferroelectric, superconductive, half-metallic and ferromagnetic, and more. In result, this class of materials provides many avenues to the realm of materials by design.

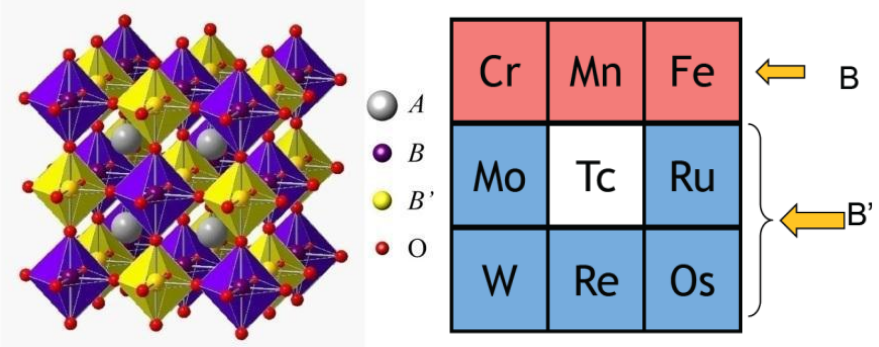

Figure 2.1: Double perovskite crystal structure (left) and possible choices for B/B' site elements (right).

Half-metallic ferromagnetic materials, such as Sr_2FeMoO_6, are of high interest in technological materials research because they can be used in devices utilizing spintronics such as read/write heads and magnetic sensors, magnetic random access memory (MRAM) devices, and spin injectors. These kinds of devices are shown in Figure 2.2.

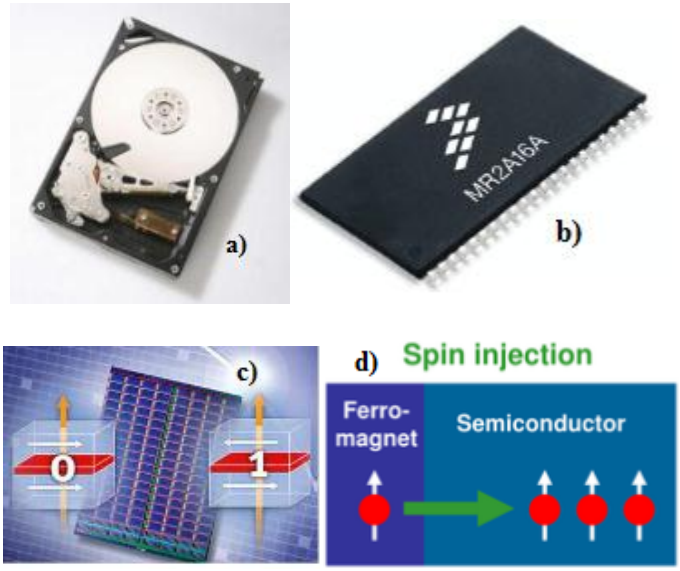

Figure 2.2: a) Read/write head b) MRAM device c) Magnetic Tunnel Junction d) Spin injector.

Magnetic tunnel junctions (MTJs) are interesting heterostructures because by using materials with near ideal spin polarization (100%), MTJs can exhibit extremely high magnetoresistance. A schematic of an MTJ is shown in Figure 2.3.

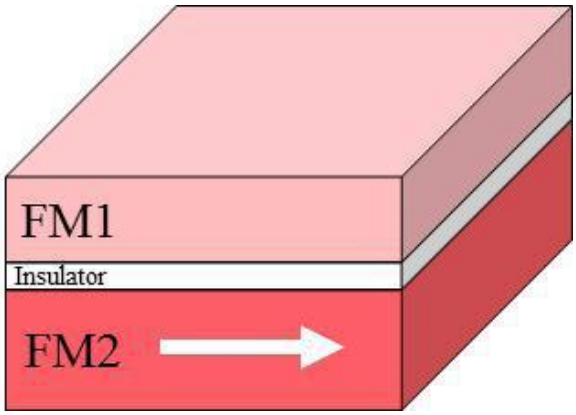

Figure 2.3: Schematic of a magnetic tunnel junction.

The magnetoresistance of a magnetic tunnel junction like the one shown in Figure 2.3 is given by the equation

$$MR = \frac{2P_1P_2}{(1 - P_1P_2)}$$

where P_1 and P_2 are the spin polarizations of layers 1 and 2, respectively. Half-metals exhibit theoretical 100% spin polarization (P = 1), so the use of half-metallic ferromagnetic double perovskites can theoretically drive the MR to an infinite value, which is desirable for MTJs. In the real world, however, the goal is simply to fabricate materials with as high spin polarizations as possible to be used in practical MTJs with potential for very large MRs.

Sr_2FeMoO_6, a half-metallic ferromagnet, is a desirable double perovskite to study for a variety of reasons. First and foremost, general double perovskites have been studied for decades in bulk form. Until recently, however, very little research was conducted on the growth and use of epitaxial films of these materials. There is a large knowledge base for Sr_2FeMoO_6 in the bulk form, so it provides an opportunity for comparison between

the bulk material and epitaxial films. In addition, the synthesis of Sr_2FeMoO_6 is less costly than many other double perovskites. One other important property of Sr_2FeMoO_6 is its high Curie temperature of about 420 K. This allows the material to exhibit its desirable structural and magnetic properties well above room temperature.

CHAPTER 3

PROJECT PROCEDURES

The chemical reaction used to synthesize our material was as follows

$$4SrCO_3 + Fe_2O_3 + 2MoO_3 + H_2 \rightarrow 2Sr_2FeMoO_6 + 4CO_2 + H_2O$$

We first stoichiometrically combined the three reactant powders ($SrCO_3$, Fe_2O_3, and MoO_3) before heating them for reaction. An atmosphere of H_2 gas was also used to reduce the excess oxygen in the material and to remove excess impurities. The focus of this project was to maintain a constant heating procedure while varying the grinding processes of the bulk material. The grinding and heating procedure was as follows (separated into 3 phases):

General synthesis procedure:

- 1a) Grinding 1 (mix reactants)
- 1b) Heat in N_2 @ 900˚C 5hrs (calcination)
- XRD 1 (observe phase impurities)
- 2a) Grinding 2
- 2b) Heat in 5% H_2/Ar 1000˚C 10hrs (reduction)
- XRD 2 (observe phase purity)
- 3a) Grinding 3, press into target
- SEM particle sizes
- 3b) Heat in pure Ar 1275˚C 10hrs (sintering)
- XRD 3, SQUID, SEM target surfaces

For this project, 5 different Sr_2FeMoO_6 samples were used for analysis. Each of these samples experienced varying grinding procedures. The grinding procedures are shown in Table 3.1.

Sample	Grinding 1	Grinding 2	Grinding 3
A	BM 8hrs	BM 8hrs	BM 4hrs
B	BM 2hrs	BM 2hrs	BM 2hrs
C	BM 30mins	BM 30mins	BM 30mins
D	HG 2hrs	HG 2hrs	HG 2hrs
E	HG 10mins	HG 10mins	N/A

Table 3.1: Grinding procedures for 5 samples.
BM – planetary ball mill, HG – manual hand grind

Throughout the synthesis procedure, for each sample, XRD analysis was performed to monitor the phase purity. Scanning Electron Microscopy (SEM) was used after grinding 3 to observe particle sizes of the bulk. Finally, SEM was used again after sintering to observe target densities via surface imaging and Superconducting Quantum Interference Device (SQUID) magnetometry was used to observe the magnetic responses of each sample.

CHAPTER 4

RESULTS

First, we discuss XRD results. As stated previously, X-Ray Diffraction was used at three different stages of the synthesis procedure for each sample. The importance of the first and second phases of X-Ray Diffraction was to observe the relative amount of impurities in the samples after the reduction heating (second phase) when compared to just after calcination (first phase). Figures 4.1 and 4.2 demonstrate this trend, where Figure 4.1 shows the diffraction data of the 8 hour ball-milled sample after calcination (with impurities) and Figure 4.2 shows the diffraction data for the same sample after reduction (negligible impurities). The asterisks (*) mark each XRD peak corresponding to the desired Sr_2FeMoO_6 material.

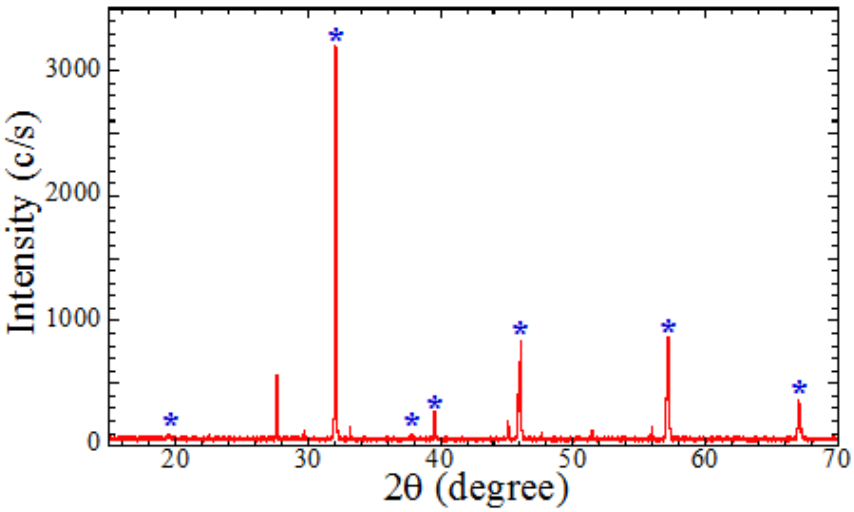

Figure 4.1: 8 hour ball-milled sample X-ray Diffraction data after calcination with impurities evident. * desired material peaks

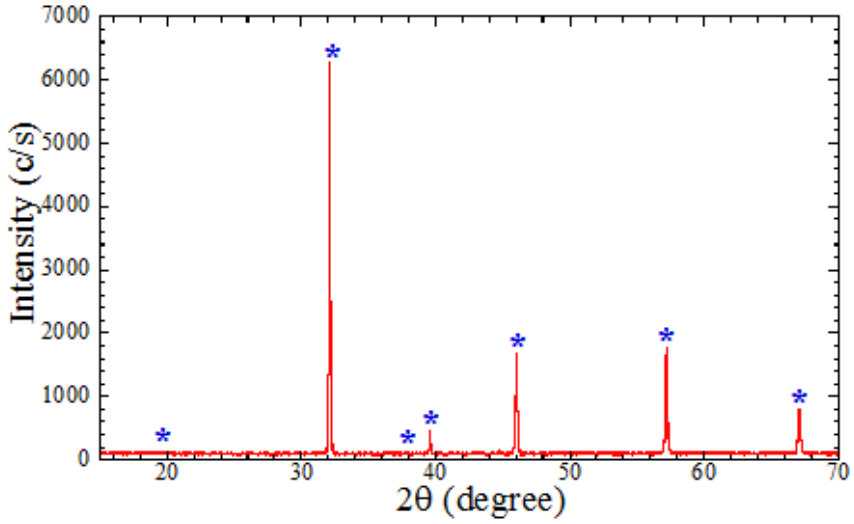

Figure 4.2: 8 hour ball-milled sample X-ray diffraction data after reduction with negligible impurities evident. * desired material peaks

The 10 minute hand-grinded sample was aborted after XRD analysis demonstrated large amounts of impurity phases after reduction had been attempted three times. The short interval of grinding for this sample was not sufficient to form small

particles, thus hindering reactions.

After the sintering heating phase, each of the samples (not including the 10 minute hand-grinded sample) was again analyzed using X-Ray Diffraction so that the ordering of the B and B' sites could be determined. Such a calculation is done using Rietveld refinement which, in essence, fits the experimental data statistically to give crystal structure and ordering parameters. One example of a Rietveld refinement fit is shown in Figure 4.3.

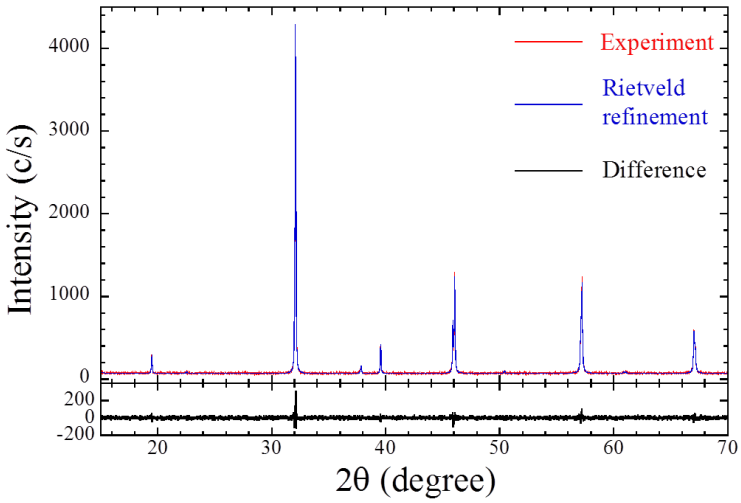

Figure 4.3: Rietveld refinement fit for the 8-hour planetary ball mill grinding sample post-sintering.

The most important parameter collected using Rietveld refinement is the ordering parameter, S. This value, for each sample, corresponds to the fraction of B and B' atoms sitting on the B and B' sites, respectively. The ordering parameter is related to this fraction by the equation

$$S = 2(f_B - 0.5)$$

which demonstrates that an ordering parameter of 0.9 corresponds to a fraction of B

atoms on B sites (rather than B’ sites) of 0.95, or 95%.

The 2 hour hand-grinded sample exhibited the highest B-B' ordering, with about 97% of the B atoms on the B sites and about 97% of the B' atoms on the B' sites (S = 0.94). However, it is important to note that the amount of bulk prepared using the 2 hour hand-grind synthesis was only 10 grams, an amount not sufficient enough for pressing targets used for magnetron sputtering. Data collected previously for a 40 gram 2 hour hand-grinded sample exhibited an ordering parameter of about 0.68. The variation in the results indicates that manual hand-grinding is inconsistent, dependent both on the experimentalists involved (and the techniques they use) as well as the amount of bulk being prepared.

Results for the 30 minute ball-milled sample indicated a B-B' ordering parameter of about 0.88 and the 8 hour ball-milled sample indicated a B-B' ordering parameter of about 0.94. The results obtained using the samples prepared by planetary ball mill indicate that the bulk material synthesized using the ball mill is much more consistent than that synthesized manually. The amount of bulk material made using the 8 hour ball-mill procedure was 30 grams, thus we can see that the ball mill was able to produce equivalent ordering to the 2 hour hand-grinded sample, but with triple the amount of material.

Next, we will look at SEM images and discuss the qualitative results. Figure 4.4 shows an SEM image of the 8 hour ball-milled sample before sintering, which shows the particle sizes of the material. Similar images were taken for the short hand-grinded, 2 hour hand-grinded, 30 minute ball-milled, and 2 hour ball-milled samples.

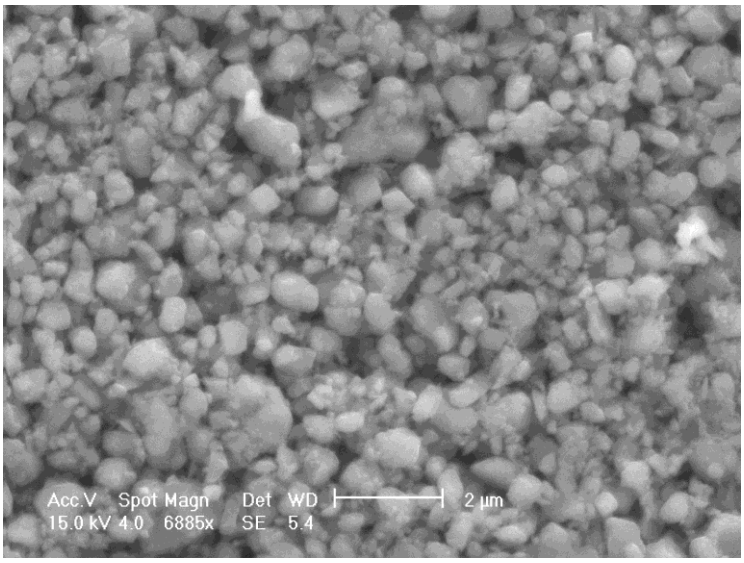

Figure 4.4: SEM image of the 8 hour ball-milled sample particle sizes before sintering.

Overall, the results of the SEM images taken before sintering demonstrated the following:

- Ball-milled samples demonstrate smaller particle sizes than do hand-grinded samples
- Ball-milled samples demonstrate smaller ranges of particle sizes than do hand-grinded samples
- An increase in length of ball-mill time decreases the particle sizes, down to a minimum limit

Quantitative analysis was also performed on the SEM images before sintering. Random lines of known length, calibrated to the scale marker on the images, were overlaid on each image, giving a total line length L. Then, the number of intersections with particle boundaries was counted. Each intersection with a boundary counted as a value of 1 and each tangent intersection counted as a value of 0.5. The total number of

intersections was noted as N. Then, the average particle length was taken as the total line length divided by the number of intersections

$$\bar{L} = \frac{L}{N}$$

Since the SEM images are 2D representations of 3D particles, a factor of 1.5 is used to convert this average particle length of the average particle diameter.

$$\bar{d} = 1.5x\bar{L}$$

These average particle diameters are tabulated later in this document in Table 5.1.

Next, the samples were imaged using SEM after sintering to observe the microstructure of the sputtering targets. Figures 4.5, 4.6, and 4.7 show the target microstructures for the 2 hour hand-grinded, 30 minute ball-milled, and 8 hour ball-milled samples, respectively. It is evident that the hand-grinded material produced a very porous target microstructure. Experimental measurements estimate this hand-grinded target to be about 70% as dense as theoretical bulk SFMO. Progression forward to the 8 hour ball-milled sample shows it is evident that the target is much denser than that of the hand-grinded sample. Indeed, experimental measurements estimate the 8 hour ball-milled target to be about 95-98% as dense as theoretical bulk SFMO. The difference in densities can be explained qualitatively through consideration of the particle sizes before sintering. The hand-grinded sample exhibited larger particles before sintering as well as a broader range of particle sizes, while the 8 hour ball-milled sample exhibited much smaller particles as well as a smaller range of particle sizes. In result, it seems that smaller and more coherent (in size) particles result in denser, more homogeneous (well ordered) sputtering targets.

Currently, our group has done little work in studying the advantages and disadvantages of porous vs. dense sputtering targets and such work may be done in the future. However, we hypothesize that denser, more well-ordered targets like that demonstrated by the 8 hour ball-milled target will result in more ideal epitaxial films via sputtering.

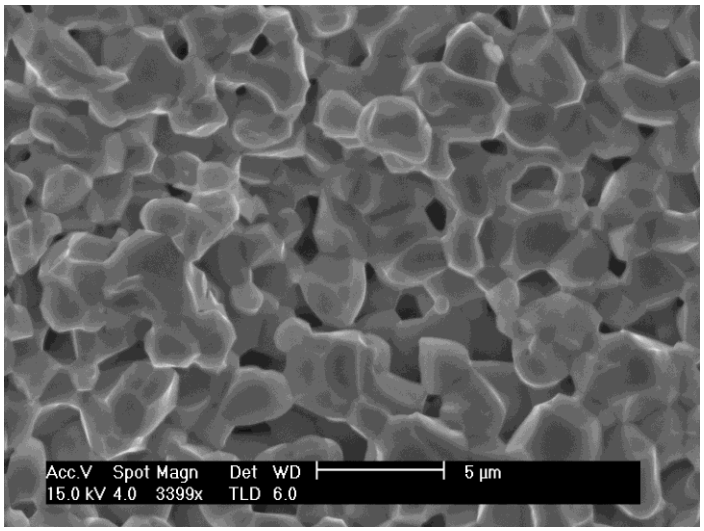

Figure 4.5: SEM image of sintered target microstructure for 2 hour hand-grinded SFMO.

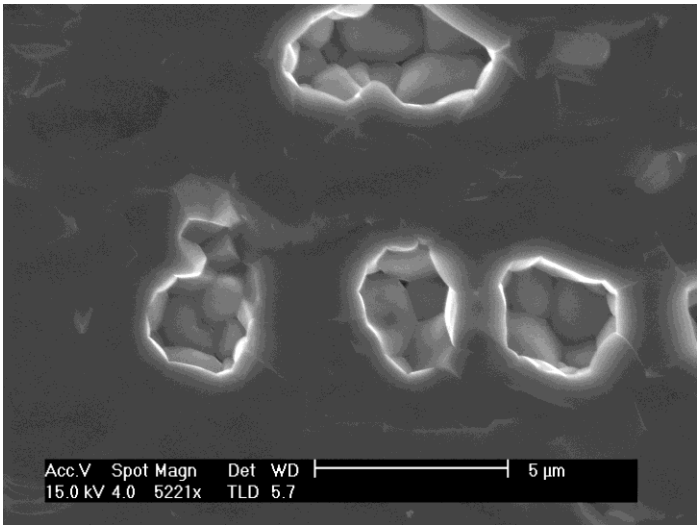

Figure 4.6: SEM image of sintered target microstructure for 30 minute ball-milled SFMO.

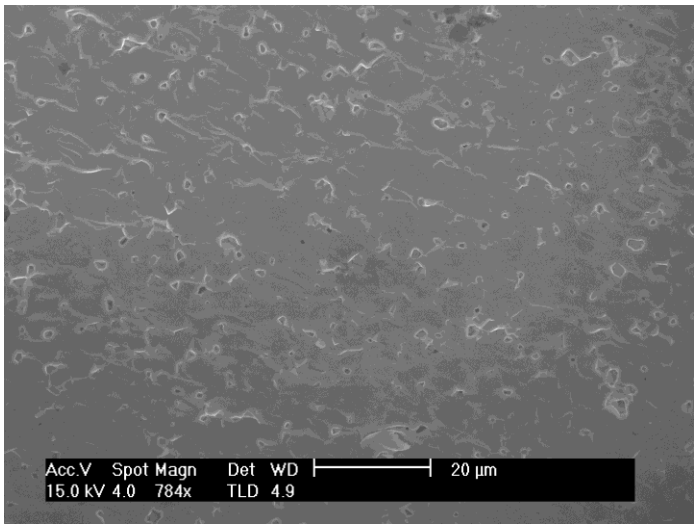

Figure 4.7: SEM image of sintered target microstructure for 8 hour ball-milled SFMO.

Lastly, we'll look at the magnetic data achieved for a few SFMO samples prepared using different synthesis techniques. In Figure 4.8, the plot shows magnetization vs. magnetic field applied for the 2 hour hand-grinded sample. Results indicate that this sample, with a 0.94 B-B' ordering parameter, exhibits a magnetization of 3.72 μB/f.u. at 5 K, where SFMO is predicted to have a magnetization of 4 μB/f.u. at 0 K. Thus, we see that this hand-grinded sample demonstrates a fantastic result in the magnetic sense, but as we mentioned earlier, this sample was only prepared at an amount of 10 grams, so the reproducibility of desirable magnetic results through manual grinding of larger bulk amounts (~40 g needed for sputtering targets) is difficult. Indeed, previous results have indicated a magnetization of about 2.70 μB/f.u. for a large batch of this material with 2 hour hand grinding.

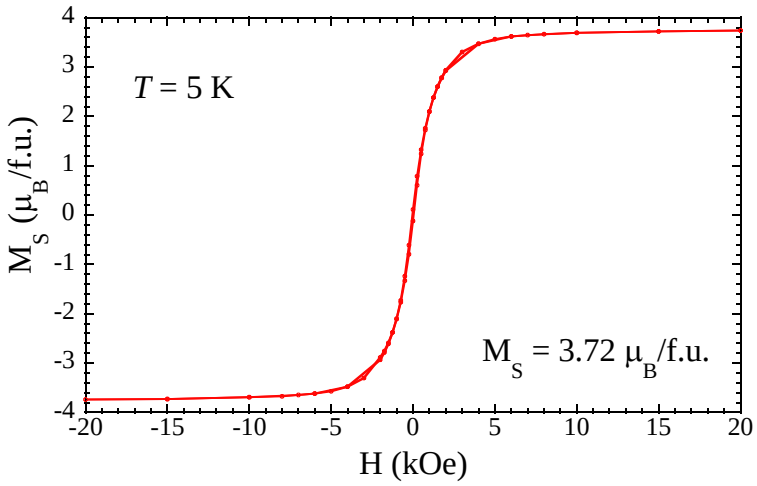

Figure 4.8: Magnetization vs. applied magnetic field for the small batch 2 hour hand-grinded sample.

Figure 4.9 shows the magnetic data achieved for the 8 hour ball-milled sample. Results indicate still a high magnetization of 3.58 μB/f.u. at 5 K, but it is obvious that this magnetization is not quite as high as the 2 hour hand-grinded sample.

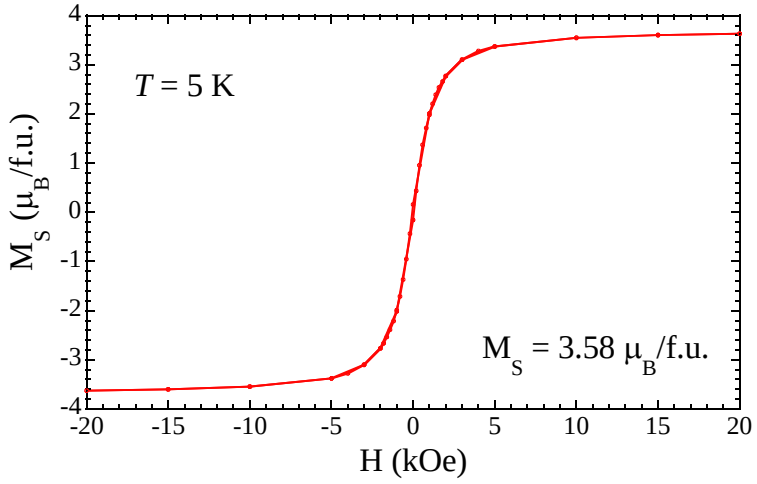

Figure 4.9: Magnetization vs. applied magnetic field for the 8 hour ball-milled sample.

There may be a few things that could cause the 2 hour hand-grinded sample to exhibit a higher magnetization than the ball-milled sample. One such reason is that the 2

hour hand-grinded sample may contain more impurities. These impurities may be magnetic phases (with a stronger magnetic response per unit volume than the bulk) which contribute to the overall magnetization of the bulk.

Figures 4.10 and 4.11 show the magnetization vs. temperature plots for the two samples discussed above.

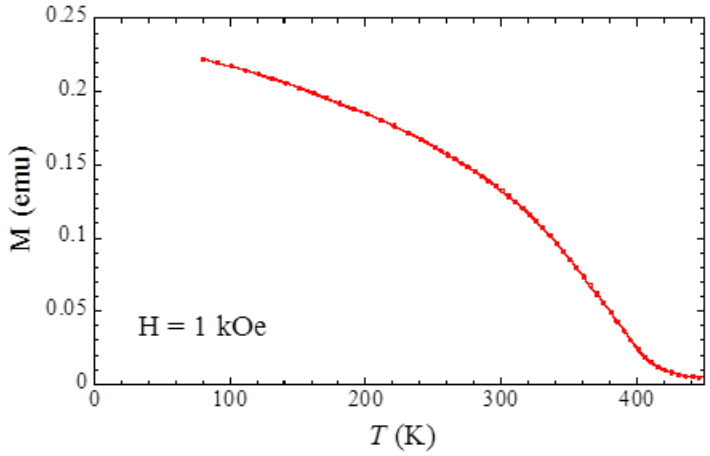

Figure 4.10: Magnetization vs. Temperature for the large batch 2 hour hand-grinded sample.

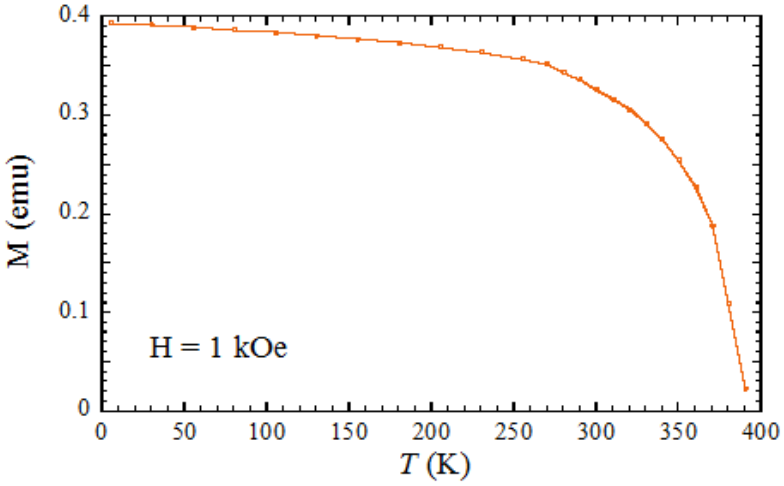

Figure 4.11: Magnetization vs. Temperature for the 8 hour ball-milled sample.

The plots of magnetization vs. temperature shown above are both for large batches of Sr_2FeMoO_6. Figure 4.10 for the 2 hour hand-grinded sample demonstrates a Curie temperature (temperature at which magnetization extrapolates to zero) of about 410 K, while Figure 4.11 for the 8 hour ball-milled sample demonstrates a Curie temperature of about 390 K. While the 2 hour hand-grinded sample exhibits a Curie temperature closer to the ideal value of 420 K, observation of the plot gives evidence that the 2 hour hand-grinded sample is less homogenous. This can be seen because the 2 hour hand-grinded data exhibits a gradual decrease in magnetization over temperature while the 8 hour ball-milled sample shows a drastic decrease in magnetization close to its ideal temperature. The 2 hour hand-grinded sample is likely demonstrating a superposition of many Curie temperatures corresponding to the various regions of order in the sample. An ideal sample would show a sudden drop in magnetization more similar to that of the 8 hour ball-milled sample.

CHAPTER 5

CONCLUSIONS

Table 5.1 summarizes the data collected from the many samples synthesized during this project.

Batch	Weight/g	Order parameter (S)	Particle Size Range/μm	Target Density/% theoretical
HG 10 min	10	------	1.195	------
HG 2 hrs*	40	0.68	0.764	~50
HG 2 hrs	10	0.94		~70
BM 30 mins	10	0.88	0.756	~85-90
BM 2 hrs	10	------	------	------
BM 8 hrs	30	0.94	0.702	~95-98

Table 5.1: Order parameters, particle sizes, and target density estimates for the bulk samples prepared during this project. * large batch ~40g

Observation of the tabulated data reveals that the bulk sample prepared by 8 hour ball mill exhibits the most desirable properties. First and foremost this sample was a larger batch of about 30-40 grams, enough for pressing a target necessary for magnetron sputtering. In addition, this sample demonstrated the highest order parameter, S, of 0.94 corresponding to 97% of B and B' atoms sitting on the B and B' sites, respectively. This sample had the smallest average particle size of 0.702 μm and post-sintering target density of about 95-98%. Lastly, this sample exhibited promising magnetic properties with a saturation magnetization of 3.58 μB/f.u. at 5 K and a Curie temperature of roughly 390 K.

The Sr_2FeMoO_6 material synthesized during this project utilizing the planetary ball mill for a time of 8 hours has proven to be the most nearly ideal bulk seen thus far by our group. Work continues to be conducted in our lab regarding application of this synthesis procedure to sputtering epitaxial films of Sr_2FeMoO_6.